Available online at www.sciencedirect.com
SCIENCE DIRECT
Polymer 47 (2006) 1333–1339
polymer
www.elsevier.com/locate/polymer

Novel regenerated cellulosic material prepared by an environmentally-friendly process

Ik Soo Kim [a], Jae Pil Kim [b], Seung Yeop Kwak [b], Yoon Soo Ko [c], Yong Ku Kwon [c,*]

[a] SK Chemicals, 600 Suwon, Kyonggi-Do 440-745, South Korea
[b] School of Materials Science and Engineering, College of Engineering, Seoul National University, Seoul 151-742, South Korea
[c] Department of Polymer Science and Engineering, Inha University, Incheon 402-751, South Korea

Received 12 May 2005; received in revised form 30 November 2005; accepted 11 December 2005
Available online 18 January 2006

Abstract

Novel regenerated cellulosic materials have been developed using an environmentally-friendly, facile process without releasing any toxic materials. Untreated, cellulose diacetate fibers were immersed in the aqueous caustic solution. The degummed and dried diacetate fibers were heated at a rate of 2 °C/min from 30 to 98 °C, then treated for 30 min at the same temperature and cooled at a rate of 2 °C/min to 30 °C, followed by the drainage of the liquid. The heat treated fibers were held under tension to prevent shrinkage during the thermal treatment. The materials possess excellent physical and dyeing properties, are pleasant to touch, and can be used in a variety of industrial fields. The microstructure of these materials is found to have a composite crystalline structure consisting of cellulose II and cellulose IV, exhibiting a lamellar morphology with an increased amorphous fraction, as compared to conventional rayon fibers, which is the main reason for their better elongation and solvent sorption ability.

Keywords: Regenerated cellulose fibers; Microstructure; Crystallinity

1. Introduction

Most of polymeric materials are synthesized from small organic molecules, which originate from the limited petrochemical resources. Due to the lack of availability of the source materials, recent researches have focused on the development of new materials which can be produced from naturally occurring polymers, such as polysaccharides, proteins, lipids and so on. The benefits of using naturally occurring polymers include their natural abundance and environmental compatibility, whereas one of the limitations to their use is the difficulty involved in their processing and fabrication, because of the polar moieties included in their backbones. One of the most attractive candidates is cellulose, which is actively used in a variety of different products. Cellulose is generally regarded as being the most abundant and useful renewable material, due to its excellent physical properties, such as its gloss, specific gravity and pleasant touch. Over the years, many researchers have attempted to find advanced cellulose derivatives combining by a number of commercial products [1].

As a typical example, rayon fiber is defined as a fiber made of a polymer of β-1,4-linked D-glucopyranose (hereinafter referred to cellulose), in which not more than 15% of the hydrogens of the hydroxyl groups have been replaced by manufacturing impurities, pigments and fire retardants [2]. Rayon fibers are usually used for high quality clothes, by virtue of their characteristic gloss, specific gravity and pleasant touch. These fibers also form the basis of high strength, high modulus fibers, because of the molecular conformation of cellulose, which is made of D-glucopyranose monomer units in the preferred chair form joined by β-1,4 glucosidic linkages [3]. One of the benefits of using rayon fibers in material applications is that they originate from a renewable resource, cellulose, which is nature's most abundant polymer, thereby providing a mean of extending the non-renewable petrochemical resources. Another benefit includes their environmental compatibility, which can alleviate the environmental problems associated with synthetic polymeric materials.

However, it was found that the regenerated cellulose fibers produced by conventional processes posed serious environmental and economical problems, thereby causing their usage in various practical applications to be contracted. Most regeneration methods of cellulosic fibers depends on solubilizing

* Corresponding author. Tel.: +82 32 860 7482; fax: +82 32 865 5178.
E-mail address: ykkwon@inha.ac.kr (Y.K. Kwon).

0032-3861/$ - see front matter © 2005 Elsevier Ltd. All rights reserved.
doi:10.1016/j.polymer.2005.12.070

cellulose, and then reshaping it into long-fibered products by extrusion through the small holes of spinnerets, immediately followed by the conversion of the extrudate into solid cellulose [3]. In the typical manufacturing processes of these wet-spun (viscose) rayon fibers, the raw material is alkali cellulose with a relatively high α-cellulose content, which is prepared by treating wood pulp with an excess of sodium hydroxide solution. This alkali cellulose is then aged to the desired degree, before undergoing oxidative depolymerization and being reacted with carbon disulfide (CS_2) to form sodium cellulose xanthate. The cellulose xanthate is cooled in dilute sodium hydroxide solution with high shear to produce the clear viscous solution, called viscose. After ripening to a certain degree of polymerization, it is extruded so as to form regenerated cellulose fibers through spinnerets. The spinning bath contains sulfuric acid as well as sodium and zinc sulfate in varying proportions.

The raw materials such as sodium sulfate and zinc sulfide, which are used in the production of the rayon fibers, are subsequently recovered. However, only 30–35% of the CS_2 used in the formation of the sodium cellulose xanthate is recovered, while the remaining CS_2 is lost through volatilization and decomposition during the spinning process. Pure CS_2 is a colorless and volatile liquid. There are no data available on the pollution caused by CS_2 on a regional or global scale, but it is known to cause serious damage to the human body upon chronic exposure. Since the main source of CS_2 emission is from plants used for the production of regenerated cellulosic materials, it is predicted that the conventional viscose rayon process will be phased out very soon. Due to the demand for comfortable clothing and functional materials with low production cost, much scientific and industrial effort has been focused on the development of methods of regenerating cellulose without the release of pollutants [3–5]. However, they are not produced owing to their high manufacturing cost and excessive stiffness.

Here, we developed a novel cellulosic material using an environmentally-friendly, facile regeneration process at an economical cost, without releasing any toxic materials. We used the untreated, cellulose diacetate fiber as a raw material and the use of toxic CS_2 and heavy metal ions were avoided in an attempt to reduce the release of toxic materials. These cellulose diacetate fibers were treated in the aqueous caustic solution for regeneration and then heated under tension to prevent shrinkage and enhance chain orientation during the thermal treatment. The microstructure of the final regenerated cellulosic material was investigated by FT-IR and X-ray diffraction and its mechanical and dyeing properties were also measured in this study. We denote the regenerated cellulosic material prepared by the present method as the regenerated cellulose fibers or films, while those prepared using the previous conventional methods are conveniently referred to rayon fibers or films.

2. Experimental section

2.1. Sample preparation

Untreated, cellulose diacetate fibers with a degree of substitution of 2.55 (combined acetic acid 56.9%) were scoured and dried. Separately, water was poured into a bath and caustic soda was added at a concentration of 31.3–40% by weight, based on the weight of the cellulose diacetate fibers. After being immersed in the aqueous caustic solution, the degummed and dried diacetate fibers were heated at a rate of 2 °C/min from 30 to 98 °C, then treated for 30 min at the same temperature and cooled at a rate of 2 °C/min to 30 °C, followed by the drainage of the liquid. The heat-treated fibers were held under tension to prevent shrinkage during the thermal treatment. Fig. 1 shows the SEM image of the cross-sections of the regenerated fibers.

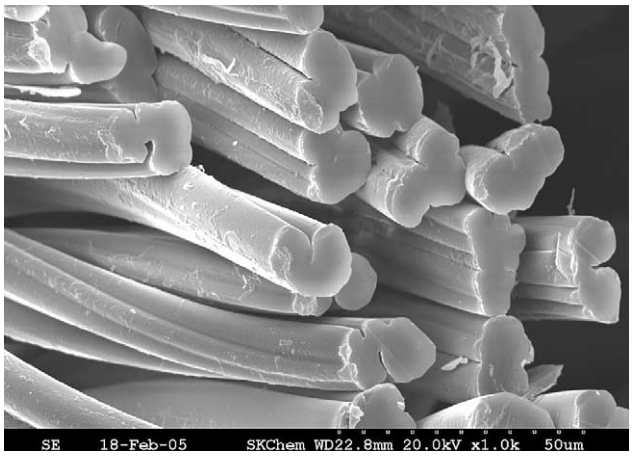

Fig. 1. SEM image of the regenerated cellulose fibers.

The same thermal treatment was repeated twice. Then, the fibers were washed with water at room temperature to remove residual alkali and dried. The final weight of the fibers was reduced by ~33 to ~40%, as compared with the initial value. The weight loss of the sample was measured using the weight change before and after the alkali treatment and calculated through the following equation: weight loss(%) = 100 × (sample weight before treatment − sample weight after treatment)/(sample weight before treatment).

2.2. Characterization

SEM measurements of the regenerated cellulose fibers were conducted on a Akashi DS130. FTIR spectra were obtained with a Nicolet, Magna 7509 spectrometer. Fibrous sample were reduced to small pieces before mixing with potassium bromide, by cutting with scissors to very short length and rolling in a mill to film-like geometry. In order to determine the structural parameters of the fibers, wide-angle X-ray diffraction (WAXD) and small angle X-ray scattering (SAXS) measurements were conducted on Beamline 4C2 at the Pohang Accelerator Laboratory, Pohang, Korea. The X-ray beam was generated from synchrotron radiation using Co Kα radiation (λ = 1.608 Å) and the storage ring was operated at an energy level of 2 GeV. The WAXD apparatus employs point focusing optics with a Si double crystal monochromator followed by an Au coated flat mirror. The sample-to-detector distance was 80 mm and the data were collected in the range of momentum transfer of $0.05 \le Q\,(\mathrm{nm}^{-1}) \le 1$, $Q = (4\pi/\lambda)\sin\theta$. The intensity

of the beam was monitored by means of an ionization chamber, in order to test for the minor decrease in the primary beam intensity during the measurements. The scattering data profiles were corrected for background and detector efficiency.

3. Results and discussion

3.1. FT-IR data

The deacetylation of the cellulose diacetate fibers was identified through their FT-IR spectra, and the spectral results are given in Fig. 2. Fig. 2 shows the FT-IR spectra of (a) the untreated cellulose acetate fibers (weight loss of 0%) and (b) the regenerated cellulose fibers (weight loss of 40.1%). In these data, the C–O stretching peak of the β-1,4-linked D-glucopyranose was read at 1160 cm^{-1}, and the carbonyl band of the acetyl groups was read at 1760 cm^{-1} [6]. These FT-IR peaks were calculated by integration and the ratio between them was obtained. In curve *a*, which corresponds to the untreated cellulose diacetate fiber, the large quantity of carbonyl groups in the acetate moieties produced the large peak at 1760 cm^{-1}. In contrast, the carbonyl peak at 1760 cm^{-1} was greatly reduced and almost disappeared in the treated, regenerated cellulose fiber (curve *b*) with a weight loss of 40%, as a result of the saponification treatment. On the other hand, the hydroxyl stretching peak at 3400 cm^{-1} intensified with increasing weight loss. On the basis of the FT-IR data, it was confirmed that almost all of the acetyl group of the untreated cellulose diacetate fibers were substituted with a hydroxyl group and that the cellulose fibers were almost completely regenerated by this treatment.

3.2. Mechanical properties of regenerated cellulose fibers

To characterize material properties of the cellulose fiber after regeneration, its modulus, elongation at break and birefringence were also measured. The tensile strength and elongation at break of the fibers were measured using a universal testing machine, using a sample 50 mm long which was stretched at a tension speed of 200 mm/min. The measured tensile strength and elongation at break of the fibers obtained before and after the treatment are summarized in Table 1. In this table, the measured tensile strength of the regenerated cellulose fiber was 1.50 gf/den, which is much higher than the corresponding value of the untreated cellulose diacetate fibers (0.68 gf/den). The higher tensile strength of the regenerated cellulose fibers is due to the substitution of the acetyl group of the cellulose diacetate fibers with a hydroxyl group which allows better molecular interaction or contact between the polymer chains through hydrogen bonding and, hence, improves the mechanical properties of the fibers.

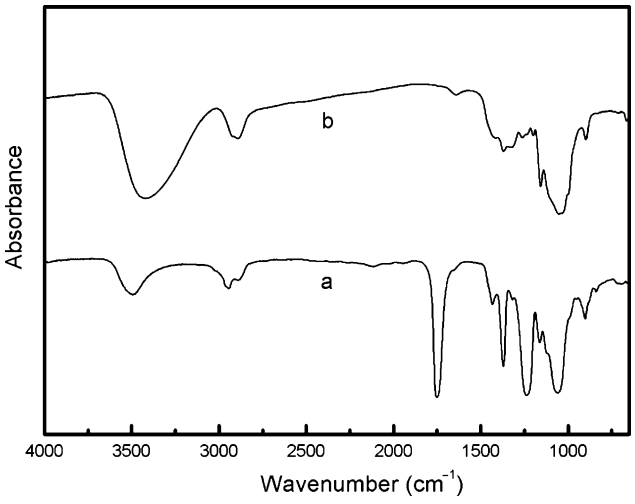

Fig. 2. FT-IR spectra of (a) the untreated cellulose acetate fibers (weight loss of 0%) and (b) the regenerated cellulose fiber (weight loss of 40.1%).

The values of elongation at break of the untreated cellulose diacetate fiber and the regenerated cellulose fiber were similar (35.5% for the untreated cellulose diacetate fiber and 36.1% for the regenerated cellulose fiber). One would expect the elongation of the regenerated fibers to be decreased, due to the enhanced chain polarity conferred on them by the saponification of the cellulose diacetate fibers. The severe thermal and mechanical treatments in the saponification stage also cause structural disorder or defects in the microstructure which may increase the elongation of the regenerated fibers.

The properties of the fibrous polymeric materials, such as their wet strength, dye uptake, moisture absorption and swelling behavior, as well as their resilience, can be controlled to a large extent by varying the processing parameters [7]. These properties are highly influenced by the microstructures of the polymeric materials, such as the relative amount of crystalline phase (crystallinity) and the chain packing or molecular orientation, especially in the intermediate phase between the crystalline and amorphous phases [8,9]. The microstructure of the fibers may be regarded as a structure in which there is a spectrum of molecular order, ranging from a highly ordered crystalline domain to a disordered amorphous region [10]. The strength originates from the crystalline material, while the amorphous material provides the flexibility, porosity and the regions generally accessible to liquids, dyes and other reagents. Therefore, the fiber properties vary depending upon the relative degrees of order and disorder in the structure (often described loosely as the crystalline/amorphous ratio) and molecular alignment (degree of orientation), i.e. a lower orientation and crystallinity mean a higher rate of dye diffusion in the fibers.

Both the crystallinity and molecular orientation strongly affect the sorption characteristics of fibrous polymers on solvent molecules [11]. Since the molecular orientation provides information on the degree of chain packing in both the crystalline and intermediate phases, birefringence measurements were conducted to measure the degree of orientation of both the untreated cellulose diacetate and the regenerated cellulose fibers. The birefringence of the fibers (Δn), calculated from the refractive indexes of polarized light which vibrated in the directions perpendicular and parallel to the axis of the fiber, respectively, were measured with the aid of a polarized microscope.

The measured Δn values of the regenerated cellulose fibers were lower than that (25.5×10^{-3}) of the untreated cellulose

Table 1
Physical properties of the regenerated cellulose and cellulose diacetate fibers

Samples	Weight loss (%)	Tensile strength (gf/den)	Elongation at break (%)	Specific gravity (g/cm^3)	Moisture regain (%)	Δn ($\times 10^3$)
Regenerated cellulose	40.1	1.41	36.1	1.50	12.1	14.2
fibers	37.5	1.30	36.1	1.49	11.2	13.9
	33.7	1.25	30.2	1.47	10.5	12.8
Cellulose diacetate fibers	0	0.68	35.6	1.31	6.5	25.5

diacetate fibers. These results indicate that the chain packing of the cellulose diacetate fibers is better than that of the regenerated cellulose fibers, which explains the better sorption property and improved elongational property of the regenerated cellulose fibers.

3.3. X-ray data

As with most synthetic and natural polymeric fibers, the mechanical properties of the fibers were largely affected by various structural parameters such as crystallinity and molecular orientation. In order to determine the structural parameters of the fibers, the XRD measurements were conducted on Beamline 4C2 at the Pohang Accelerator Laboratory, Pohang, Korea. The X-ray beam was generated from synchrotron radiation using Co Kα radiation ($\lambda=$ 1.608 Å) and the storage ring was operated at an energy level of 2 GeV. The WAXD apparatus employs point focusing optics with a Si double crystal monochromator followed by an Au coated flat mirror. The sample-to-detector distance was 80 mm and the data were collected in the range of momentum transfer of $0.05 \leq Q$ (nm^{-1}) ≤ 1, $Q=(4\pi/\lambda)\sin\theta$. The intensity of the beam was monitored by means of an ionization chamber, in order to test for the minor decrease in the primary beam intensity during the measurements. The scattering data profiles were corrected for background and detector efficiency. The fibers were aligned perpendicular or parallel to the direction of the X-ray beam, in order to obtain equatorial and meridional X-ray diffraction data, respectively. The fiber diagrams of the unoriented fibers were also measured, in order to estimate the approximate apparent crystallinity. In particular, in order to estimate the approximate crystallinities of the fibers, the empirical amorphous background and Bragg diffraction peaks in the total scattering data were separated by means of a conventional curve fitting method using commercial software. The individual peaks and amorphous background were assumed to have Gaussian-type peak profiles.

Fig. 3 shows the fiber diagram of the regenerated cellulosic fiber at room temperature. The data contain an amorphous halo with several crystalline Bragg peaks. The amorphous halo in the data was more intense than that observed in the case of the conventional rayon fibers, such as viscose rayon and cupraammonium rayon fibers, which reveals that the regenerated cellulose fiber contains a significant amount of amorphous, disordered phase in the microstructure. However, the numbers and positions of the Bragg peaks in this pattern are quite similar to those of the conventional rayon fibers, indicating that the crystalline structure of the regenerated cellulose fiber is similar to that of the conventional rayon fibers. However, it is evident in Fig. 3 that the peak width along the azimuthal direction for the regenerated cellulose fiber is much broader than that of the conventional rayon fibers. This clearly indicates that the molecular orientation of the crystalline phase of the regenerated cellulose fibers is much worse than that of the conventional rayon fibers. The larger amorphous content and poor crystalline orientation of the regenerated cellulose fiber as compared with the conventional rayon fibers arise from the severe thermal and mechanical treatments employed in the processing. This may be partially due to the amorphous nature of the cellulose diacetate fibers used as the starting material.

Regarding the crystalline structure of cellulose fibers, it is known to be classified into four crystalline types, viz. cellulose I, II, III and IV, and their crystalline structures are able to be transformed from one type to another [12,13]. The crystalline structure of cellulose I is a native form, while that of cellulose II is transformed from that of cellulose I by mercerizing it with sodium hydroxide (NaOH) [13]. The crystalline structures of cellulose III and cellulose IV are obtained from cellulose I and II by treating them with ethylamine and ethylene diamine, respectively. It was reported that the degree of crystallinity was in the order of cellulose I > cellulose IV > cellulose II > cellulose III, while the order density in the amorphous region

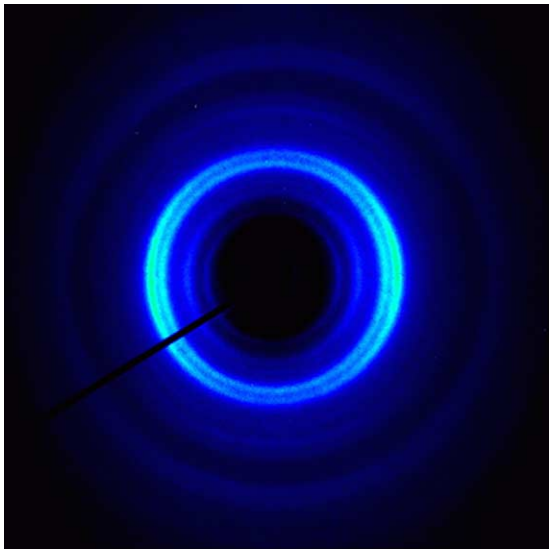

Fig. 3. Fiber diagram of the regenerated cellulosic fiber at room temperature. The fiber axis was in the vertical direction.

was in the order of cellulose I > cellulose II > cellulose III > cellulose IV, and that the tensile properties of the cellulose fibers were dependent on the crystalline structure type [14]. According to the literature, spun cellulose acetate fibers were drawn and saponified with alkali to produce rayon fibers having a cellulose II crystalline structure [4].

Fig. 4 depicts a typical one-dimensional X-ray diffractogram of the regenerated cellulose fibers, measured at room temperature. The fiber specimens were chopped and molded to remove the preferential orientation of the fibrous material. In this pattern, the non-crystalline part was taken as that contributing to the intensity of the diffuse background and the crystalline peaks as that contributing to the intensity of the selectively diffracted radiation (the peaks occurring on top of the background). In Fig. 4, both the amorphous backgrounds and the Bragg peaks were resolved by the curve fitting method. In these data, we found three strong Bragg peaks at $2\theta \approx 12$, 19 and 22 ° which were indexed as the (101), (10$\bar{1}$) and (002) peaks of the cellulose II crystal structure, respectively. It is known that the crystal structure of cellulose II is transformed from that of cellulose I, the native form of cellulose crystal, by mercerizing it with NaOH [15,16]. The unit cell parameters of cellulose II have been reported to be $a = 8.01$ Å, $b = 8.01$ Å, $c = 10.36$ Å (fiber axis), $\gamma = 117.1°$ (monoclinic). Higher order peaks were also observed in the region of $30 < 2\theta$ (degree) ≤ 60. It is known that conventional rayon fibers, such as Viscose rayon, Cupraammonium rayon, Bemberg rayon high tenacity rayon, Fortisan, Polynosic, Tyre-cord rayon, and cellophane have a crystalline structure of the cellulose II type [4,5].

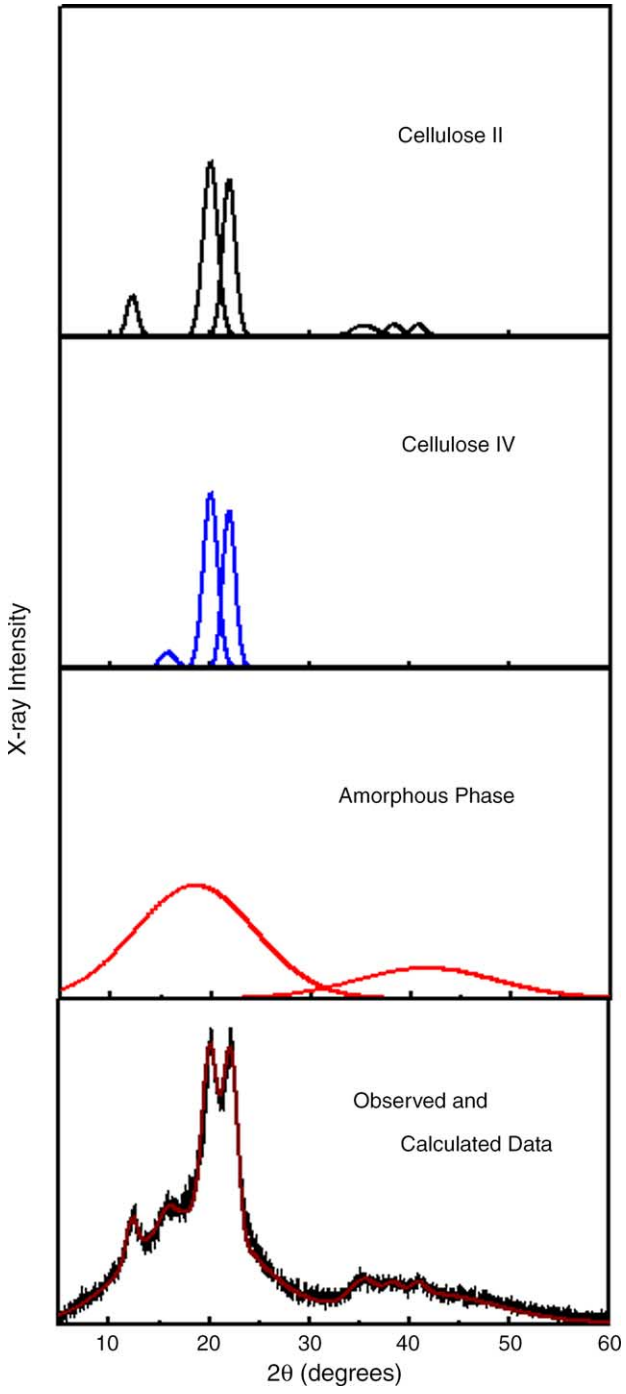

Fig. 4. Typical one-dimensional X-ray diffractogram of the regenerated cellulose fiber, measured at room temperature.

In Fig. 4, we found another peak at $2\theta \approx 15.4°$ which is the (1$\bar{1}$0) peak of the cellulose IV phase. As described above, it is known that the crystal structure of cellulose IV is obtained from that of either cellulose I or II by treating it with ethylene diamine [12,13]. Ishikawa et al. reported that the degree of crystallinity was in the order of cellulose IV > II, whereas the order of density in the amorphous region was in the order of cellulose II > IV [14]. It was also suggested that the tensile properties of cellulose fibers were affected by the type of crystal structure. The peaks at $2\theta \approx 22$ and 35° were attributed to the (020) and (040) peaks of cellulose IV which were overlapped with (002) and (004) peaks of cellulose II, respectively. The unit cell parameters of the cellulose IV crystal have been reported to be $a = 8.12$ Å, $b = 10.03$ Å, $c = 7.99$ Å (fiber axis) (orthorhombic). The coexistence of the Bragg peaks from cellulose II and IV for the regenerated cellulose fibers indicates the bimorphic behavior of the crystalline structure.

3.4. Crystallinity measurement

Since most of the crystalline Bragg peaks of the regenerated cellulose fibers were located in the region of $2\theta \leq 60°$, their approximate apparent crystallinity was estimated based on the curve fitted data shown in Fig. 4. The estimated value of crystallinity for the regenerated cellulose fibers was $28 \pm 2\%$ which was much lower than those of the conventional rayon fibers (36–51%). The lower crystallinity or higher amorphous fraction of the regenerated cellulose fiber, as compared to that of the conventional rayon fibers, is the reason for the better elongation and solvent sorption ability of the regenerated fiber.

In order for them to be used for high quality clothes, the dyeing property of the fibers needs to be considered as well. The different dyeing rates brought about by the differences in the physical structure are clearly of practical importance. One would expect the regenerated cellulose fibers to show faster exhaustion behavior than the conventional rayon fibers,

presumably due to their lower crystallinity values and poorer molecular orientation. In all types of cellulose fiber, there are 'crystalline' regions (with high parallelism of the cellulose chains) and 'non-crystalline' regions (where the chains are disordered to some extent). The parallel chains in the crystalline regions are linked together by hydrogen bonds between the OH groups of the cellulose. The crystallites lie preferentially parallel to the fiber axis and are separated by regions of lower order and intermicellar spaces. The average size of the crystallites and the quantitative ratio of crystallites to regions of lower order are strongly fiber-specific. Only the water-swollen intermicellar spaces and regions of lower order of the fiber are accessible to the large direct dyes molecules. It is completely impossible for a dye to diffuse into the highly oriented crystallites. Dyeing, therefore, only proceeds at the outer walls of the crystallites and in the non-oriented cellulose.

It is clear that our treatment of the cellulose acetate fiber or film causes the regenerated cellulosic materials to have a composite crystalline structure of cellulose II and IV. The relative ratio between cellulose II and IV in the microstructure of the regenerated cellulose fiber can be estimated based on the approach used to measure the apparent crystallinity in Fig. 4. Here, we again assume that most of the crystalline Bragg peaks were located in the region of $2\theta \leq 60°$, and the approximate apparent amounts of each crystalline phase were estimated based on the curve fitted data shown in Fig. 4. The result is displayed in Fig. 4. Since the peaks at $2\theta \approx 15.4$, 22 and 35° [$(1\bar{1}0)$, (020) and (040) peaks, respectively] occur due to the crystal structure of cellulose IV, we can estimate the relative amount of the cellulose IV crystal in the microstructure from this data. In Fig. 4, the peak at $2\theta \approx 15.4°$ occurred only due to cellulose IV. However, the peaks at $2\theta \approx 22$ and 35° of cellulose IV were overlapped with the (002) and (004) peaks at $2\theta \approx 22$ and 35°of the cellulose II crystal. The separation of these peaks from the cellulose II peaks was carried out based on information provided in the literature [17]. It has been reported that the areas of the peaks at $2\theta \approx 15.4$, 22 and 35° of cellulose IV are approximately in the ratio of 1:2.5:1.3. Assuming that the peaks from the cellulose IV crystal in the microstructure of the regenerated cellulose fiber follow these proportions, the peaks at $2\theta \approx 22$ and 35° were resolved for the peaks of cellulose II and IV, as shown in Fig. 4. Based on the peak separation procedure, we estimated the relative proportion of the cellulose IV crystal in the crystalline phase to be approximately 17%.

Our small angle X-ray scattering data of the regenerated cellulose fiber, as shown in the curve *a* of Fig. 5, showed a SAXS peak at $Q \approx 0.42$ (nm^{-1}) which corresponded to a long period of ~15 nm whereas the SAXS peak intensity of the conventional rayon fibers (Fig. 5(b)) was scarcely visible. The absence of the SAXS peak for the conventional rayon fibers indicates that their chains were highly extended and that the crystal morphology was similar to that thought to exist in the extended chain crystal. On the other hand, the presence of the SAXS peak with a long period of ~15 nm may be due to the crystal morphology being one of lamellar crystals, which is one observed in a number of conventional synthetic polymers. In the lamellar morphology of the crystal phase of the regenerated cellulose fiber, the amorphous phase was located between the lamellar crystals and, therefore, it was more elongated than that of the conventional rayon fibers when they were subjected to the elongation.

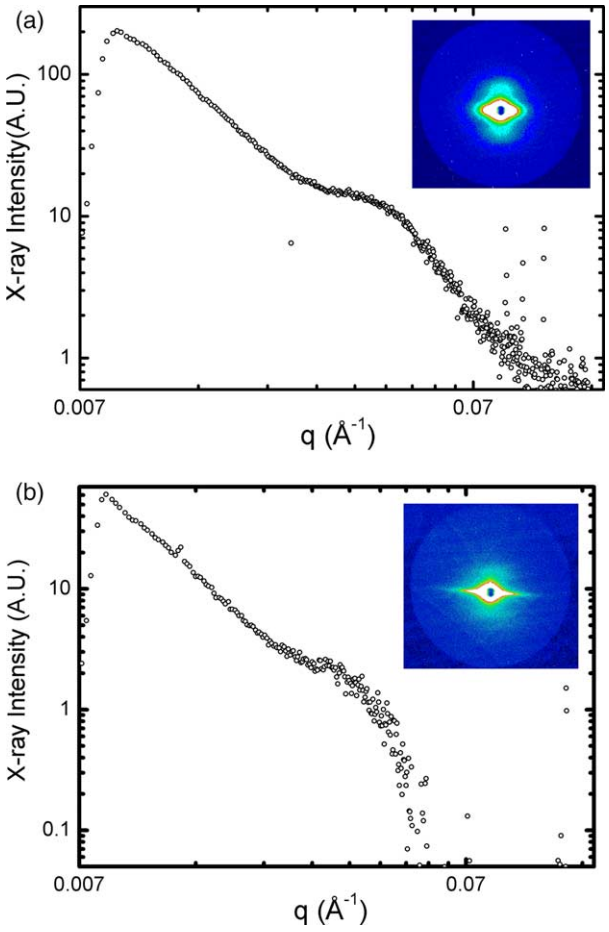

Fig. 5. Typical one-dimensional SAXS data of (a) the regenerated cellulose fibers and (b) conventional rayon fibers, measured at room temperature. The insets represent the corresponding two-dimensional SAXS pattern. The scanning direction was on the meridian of the pattern.

4. Conclusion

The method we proposed in this report produced a novel regenerated cellulose fiber in which a cellulose II crystalline structure coexists with a cellulose IV crystalline structure. The advantage of the proposed method is its simplicity, and low production cost. Unlike conventional methods of producing viscose rayon which use highly concentrated alkali solutions, CS_2 and H_2SO_4, the proposed method dose not produce serious pollutants. Another advantage of the proposed method lies in the fact that various cellulose acetate products can be used employed to produce the regenerated cellulose products in an environmentally-friendly and simple process.

Acknowledgements

Funding for this work was provided by research grant from the Korea Science and Engineering Foundation (KOSEF) through the Optics and Photonics Elite Research Academy (OPERA), an official KOSEF-created engineering research center (ERC) at Inha University, Korea.

References

[1] Vigo TL. Cellulose derivatives. In: Mark HF, Bikales NM, Overberger CG, Menges G, editors. Encyclopedia of polymer science and engineering. New York: Wiley; 1985.
[2] In Rules and Regulations under the Textile Fiber Products Identification Act, US Federal Trade Commission.
[3] Moncrieff W. Man-made fibers. London: Newnes-Butterworths; 1975.
[4] Schurz J, Lenz J. Macro Symp 1994;83:273–89.
[5] Kumar A, Harnden A. Text Chem Color 1994;26:25–8.
[6] Carrillo A, Colom X, Sunol JJ, Saurina J. Eur Polym J 2004;40: 2229–34.
[7] Lemstra PJ, Kirschbaum R, Ohta T, Yasuda H. Developments in oriented polymers-2. In: Ward IM, editor. London: Elsevier; 1987.
[8] Kwon YK, Boller A, Pyda M, Wunderlich B. Polymer 2000;41: 6237–49.
[9] Fu YG, Annis B, Boller A, Jin YM, Wunderlich B. J Polym Sci, Polym Phys 1994;32:2289–306.
[10] Fu YG, Busing WR, Jin YM, Affholter KA, Wunderlich B. Macromolecules 1993;26:2187–93.
[11] Strnad S, Kreze T, Stana-Kleinschek K, Ribitsch V. Mater Res Innovations 2001;4:197–203.
[12] Marrinan HJ, Mann. J Polym Sci 1956;21:301–11.
[13] Jung HZ, Benerito RR, Berni RJ, Mitcham DJ. Appl Polym Sci 1977;21: 1981–8.
[14] Ishikawa A, Okano T, Sugiyama J. Polymer 1997;38:463–8.
[15] Kolpak F, Blackwell J. Macromolecules 1976;9:273–8.
[16] Stipanovic AJ, Sarko A. Macromolecules 1976;9:851–7.
[17] Segal L. J Polym Sci 1961;55:395–409.